MULTIBODY DYNAMICS 2007, ECCOMAS Thematic Conference
C.L. Bottasso, P. Masarati, L. Trainelli (eds.)
Milano, Italy, 25–28 June 2007

MULTIDISCIPLINARY APPROACH TO RAILWAY PNEUMATIC SUSPENSIONS: PNEUMATIC PIPE MODELLING

Nicolas Docquier⋆[1], **Paul Fisette**⋆ **and Hervé Jeanmart**†

⋆Center for Research in Mechatronics
Université catholique de Louvain, Place du Levant 2, 1348, Louvain-la-neuve, Belgium
e-mails: `nicolas.docquier@uclouvain.be`, `paul.fisette@uclouvain.be`

†Unité de thermodynamique
Université catholique de Louvain, Place du Levant 2, 1348, Louvain-la-neuve, Belgium
e-mail: `jeanmart@term.ucl.ac.be`

Keywords: pneumatic suspension, multibody dynamics, multiphysics modelling.

Abstract. *On the majority of modern railway vehicles, airspring are used for the secondary suspension, i.e. the suspension located between the bogie frame and the carbody. The airspring is connected with several other pneumatic components such as auxiliary tanks, pipes, valves, etc. Such a system can be analysed in a multidisciplinary approach by coupling a multibody model of the train with a detailed pneumatic model of the suspension. This paper presents and compares various modelling approach for the pneumatic suspension, focusing on the bellow-pipe-tank subsystem. The pipe is described in more details distinguishing models with algebraic or differential equations and models that take compressible effects into acount or not. The various approaches are compared on a simple excitation test and confronted to a reference solution obtained with the commercial FLUENT software. It is shown that the compressible effect can not always be neglected. The influence of the pipe length is also presented.*

[1]FNRS Research Fellow.

1 INTRODUCTION

Nowadays, the modelling of mechatronic systems often requires a multidisciplinary approach. This is especially the case for railway and ground vehicles. In many cases, this implies the use of multibody dynamics but also other disciplines such as fluid mechanics, electrical circuits and actuation. For instance, Ref. [1] analyses a railway bogie with a three-phase motor coupling multibody and electrical models while Ref. [2] investigates the "multibody-hydraulic" coupling for a new car suspension system.
Another application is the secondary suspension of a railway vehicle which consists of airsprings on the majority of modern passenger trains. In addition to the pneumatic bellows, the system contains various pneumatic components such as tanks, pipes, orifices, levelling valves, the purpose of the latter being to maintain a constant height between the carbody and the bogie. Fig. 1 illustrates a possible combination of the various pneumatic components integrated in a simplified bogie structure.

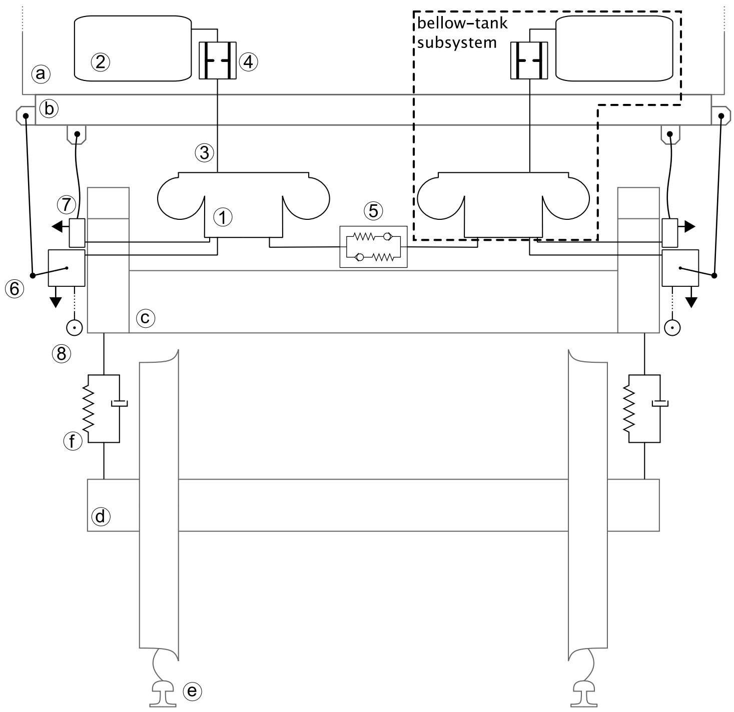

Pneumatic components
1 Bellow
2 Auxiliary tank
3 Pipe
4 Pipe orifice
5 Differential pressure valve
6 Levelling valve
7 Safety valve
8 Pressure source

Multibody components
a Carbody
b Bolster
c Bogie frame
d Wheelset
e Track
f Primary suspension

Figure 1: Example of a simplified bogie model and the various components of its pneumatic suspension.

From a modelling point of view, such a vehicle requires simultaneous multibody and pneumatic approaches. On the one hand, the carbody, the wheelsets and the bogie frames constitute a multibody system that can be modelled using multibody formalisms and programs, including the issue of wheel/rail contact. On the other hand, the modelling of the pneumatic circuit must be able to "capture" the most important phenomena in terms of dynamic response, events (valve opening, closing), etc., while being computationally efficient in a multibody co-simulation approach. The interactions between the multibody pneumatic models appear in Fig. 1: the pneumatic model calculates the bellow reaction force for a bellow crushing given by the multibody model. Furthermore, the relative motion between the bolster and the bogie frame actuates the valve lever which induces air flow in the pneumatic circuit and thus influences the airpsring reaction force.
In order to analyse the behaviour of a complete railway car, the mechanical model is im-

plemented in the multibody software SIMPACK and coupled with the pneumatic model in SIMULINK using the co-simulation interface.

Regarding the pneumatic circuit, several airspring models exist in the literature such as "equivalent mechanical" model (see Ref. [3]) or "oscillating air mass" model (see Ref. [4]). They are well appropriate for the subsystem composed of a bellow connected to a tank via a pipe with a possible damping orifice (see Fig. 1) but it is difficult or impossible to take valves and other components into account. Therefore, the description of the *complete* pneumatic circuit implies the use of thermodynamics and fluid mechanics models which take into account the airflow through pipes and valves, the pressure in the bellows, etc. These types of models are proposed in Ref. [5] and compared with other existing models.
As a first step in the model refinement, the present paper focuses on the pipe model keeping in mind that it must be integrated into the complete pneumatic circuit model. The comparison of various models made in Ref. [5] highlights the differences between models which use a differential equation to describe the pipe air motion and those which are purely algebraic. If the bellow and the tank are separated by a single orifice or by a short pipe, an algebraic model is sufficient. However, for a longer pipe, the pipe dynamics are no longer negligible and should be taken into account using a differential model.
However, the models compared in Ref. [5] assume that compressible effects in the pipe are negligible. The present paper reveals that this hypothesis is not always satisfied and shows how a better estimation of the air flow characteristics can be obtained using the Fanno's model which is a steady state solution for one-dimensional compressible flow with friction. This model is compared with the simpler models presented in Ref. [5] and confronted with reference results obtained from an axisymmetric model of the bellow-tank subsystem implemented in FLUENT.

In the first section, we introduce the various "bellow-tank" subsystem modelling approaches. Thermodynamical models are described in more details, focusing on the pneumatic pipe equations. They are then compared on a simple excitation test and confronted to the FLUENT results. We first show the frequency excitation effects before analysing the influence of the pipe length.

2 BELLOW-TANK SUBSYSTEM MODELLING

The major component of the pneumatic suspension is the bellow, which is often connected via a pipe to an auxiliary tank. Many models already exist for this subsystem, some of those have already been incorporated in multibody software as "force element". However, they do not incorporate other components such as valves and therefore, other approaches have to be used to analyse more general pneumatic configuration. In this section, we first present two "monolithic" models specifically dedicated to the "bellow-tank" subsystem. We then introduce models specific to each component and focus on the pneumatic pipe for which we distinguish models with algebraic or differential equations on the one hand, and model which take into account compressible effects on the other hand.

2.1 Monolithic bellow-tank models

"Equivalent mechanical" model This first model likens the airspring to a spring-mass system with a non-linear damper in serie and a second spring in parallel (see Fig. 2). This model presented in more detail in Ref. [3] also takes into account the friction behaviour of rubber. The

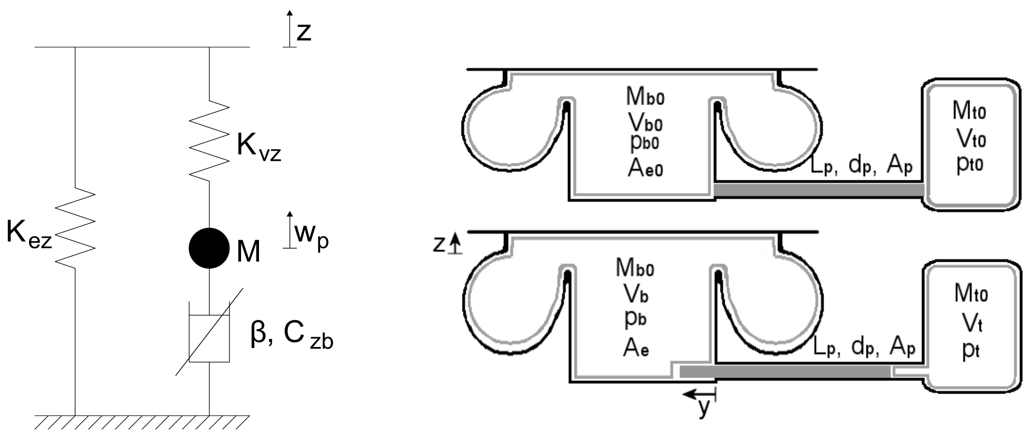

Figure 2: Left: illustration of the “equivalent mechanical” model. Right: illustration of the SIMPACK model.

effect of the pipe air mass is modelled by the mass M and the non-linear damper: it is suggested in [3] to take a damping term proportional to $\dot{w}_p{}^{\beta}$ where w_p is the mass displacement and β has a value between 1 and 2.

Oscillating air mass model The SIMPACK software (see documentation for the force element FE 82 in Ref. [4]) proposes an airspring model similar to those presented in Fig. 2: it consists in considering the air in the pipe as a constant moving mass and calculating its position and velocity by solving its equation of motion:

$$m_p \ddot{y} + \frac{\rho_p}{2} \left(\lambda \frac{L_p}{d_p} + \zeta \right) A_p \dot{y}^2 sign(\dot{y}) + (p_b - p_t) A_p = 0 \ , \tag{1}$$

with: m_p, the air mass in the pipe $[kg]$;
ρ_p, the air density $[kg/m^3]$;
y, the air mass displacement $[m]$;
$\dot{y}$, the air mass velocity $[m/s]$;
$\ddot{y}$, the air mass acceleration $[m/s^2]$;
L_p, the pipe length $[m]$;
d_p, the pipe diameter $[m]$;
A_p, the pipe section $[m^2]$;
λ, the distributed pressure drop coefficient $[-]$;
ζ, the lumped pressure drop coefficient $[-]$;
p_b, the bellow pressure $[Pa]$;
p_t, the tank pressure $[Pa]$.

The air motion induces volume variations in the bellow and the tank and therefore causes pressure fluctuations given by the isentropic equation:

$$pV^{\gamma} = p_0 V_0^{\gamma} \ , \tag{2}$$

where: V is the volume of the bellow or the tank $[m^3]$;
p is the pressure of the bellow or the tank $[Pa]$;
subscript 0 refers to initial conditions;
γ is the Poisson coefficient.

The reaction force of the bellow, which is an input of the multibody model in a co-simulation approach, can be calculated by:

$$F = A_e(p_b - p_a) \; , \tag{3}$$

where p_b is the (absolute) pressure in the bellow $[Pa]$;
p_a is the atmospheric pressure $[Pa]$;
A_e is the bellow effective area $[m^2]$.

2.2 Component specific model

The main drawback of the above formulations is that they are difficult or impossible to connect with models of the other pneumatic components illustrated in Fig. 1. In the following sections, we therefore propose to use one model for each component such as the bellow, the tank, the pipe, etc. and then to connect them with each other. We first focus on the bellow and the tank model before presenting various pipe models.

2.2.1 Bellow and tank

The bellow and the tank are modelled as pneumatic chambers in which the mass, the temperature and the pressure vary because of the flow coming from the connected pipes or from the valves.
The continuity equation imposes that the air mass variation with time is directly given by the total mass flow rate entering the chamber:

$$\frac{dM}{dt} = \dot{M} = \sum_i q_i \; , \tag{4}$$

where: M is the mass in the chamber;
q_i is an entering mass flow through port i.

The temperature variation is deduced from the internal energy variation using the first law of thermodynamics applied to an open system:

$$\frac{dT}{dt} = \dot{T} = \frac{\gamma - 1}{RM}\left(\sum_i q_i h_i - \frac{RT}{\gamma - 1}\sum_i q_i + \frac{dQ}{dt} - p\frac{dV}{dt}\right) \; , \tag{5}$$

where: T is the temperature in the chamber;
$q_i h_i$ is the total enthalpy flow rate at each pipe or valve connection;
dQ/dt is the heat flow rate;
p is the pressure in the chamber;
V is the volume of the chamber;
γ is the Poisson coefficient;
R is the perfect gas constant.

In the case of the tank, the volume variation with time, dV/dt, vanishes.
Given the temperature and the mass in the chamber, the pressure is deduced assuming a perfect gas situation:

$$pV = MRT \; . \tag{6}$$

For the bellow, the reaction force can be calculated by Eq. 3.
This approach allows us to connect several components to the bellow or the tank simply by considering several mass flows entering in the chamber. In the case of the bellow-tank subsystem,

we therefore have to calculate the mass flow rate in the pipe as a function of the bellow and tank pressures and temperatures.

2.2.2 Pneumatic pipe

Incompressible algebraic model The first approach consist in assuming that the mass flow rate is given by the steady state solution of a one-dimensional incompressible flow that passes through a pipe between two reservoirs maintained at constant pressure. As explained in Ref. [5], we can compute the pipe mass flow rate as follow:

$$q_{tb} = \sqrt{\frac{2\rho_p A_p^2}{\frac{\lambda L_p}{d_p} + \zeta} |p_t - p_b| sign\left(p_t - p_b\right)} \ , \tag{7}$$

with: q_{tb}, the mass flow rate in the pipe $[kg/s]$;
ρ_p, the air density $[kg/m^3]$;
L_p, the pipe length $[m]$;
d_p, the pipe diameter $[m]$;
A_p, the pipe section $[m^2]$;
λ, the distributed pressure drop coefficient $[-]$;
ζ, the lumped pressure drop coefficient $[-]$;
p_b, the bellow pressure $[Pa]$;
p_t, the tank pressure $[Pa]$.

Incompressible differential model Since the density ρ_p is assumed constant in this model, by taking $q_{tb} = \rho_p A_p \dot{y}$ in Eq. 1, one obtains a flow equation that take into account the pipe dynamics:

$$\dot{q_{tb}} = \frac{A_p}{L_p}\left((p_t - p_b) - \frac{1}{2\rho_p A_p^2}\left(\frac{\lambda L_p}{d_p} + \zeta\right) q_{tb}^2 sign(q_{tb})\right) \ . \tag{8}$$

Let notice that this equation is related to the incompressible algebraic model by:

$$\dot{q_{tb}} = \frac{\lambda}{2\rho A_p d_p}\left(q_{alg}^2 sign(p_t - p_b) - q_{tb}^2 sign(q_{tb})\right) \ , \tag{9}$$

where q_{alg} denotes the flow obtained by Eq. 7.

Fanno line model Contrary to above approaches, the Fanno line model takes into account compressible effects in the pipe assuming a one-dimensional adiabatic steady flow. As depicted in Fig. 3, a convergent nozzle connects the duct to an upstream reservoir maintained at a constant pressure p_0. On the other extremity, the pipe exhausts to a second reservoir maintained at a constant pressure $p_2 < p_0$.

The flow in the nozzle is supposed to be isentropic so that the pressure, the temperature and the Mach number (M) at the nozzle end (point 1) obey the following relations:

$$\frac{T_0}{T_1} = 1 + \frac{\gamma - 1}{2} M_1^2 \ , \tag{10}$$

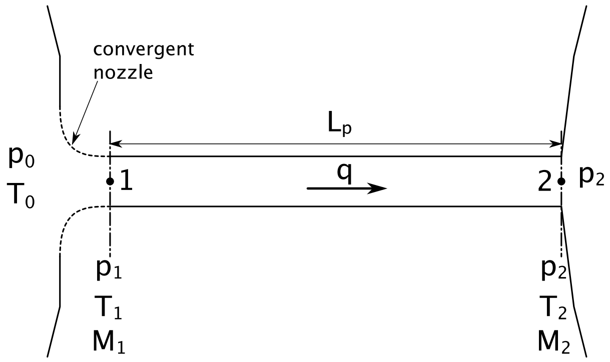

Figure 3: Illustration of the Fanno model: the pipe is connected to the upstream reservoir on the left via a convergent nozzle and directly to the downstream reservoir on the right.

$$\frac{p_0}{p_1} = \left(\frac{T_0}{T_1}\right)^{\frac{\gamma}{\gamma-1}} = \left(1 + \frac{\gamma-1}{2} M_1^2\right)^{\frac{\gamma}{\gamma-1}} \ . \tag{11}$$

From point 1 to point 2, the flow is assumed adiabatic but friction is not neglected and therefore we can deduce the following equations (see Ref.[6] and Ref.[7] for more details):

$$\frac{4C_f L_p}{d_p} = f\left(M_1\right) - f\left(M_2\right) \ , \tag{12}$$

where $f(M)$ is given by:

$$f\left(M\right) = \frac{1}{\gamma}\left(\frac{1-M^2}{M^2} + \frac{\gamma+1}{2} log\left(\frac{\frac{\gamma+1}{2}M^2}{1+\frac{\gamma-1}{2}M^2}\right)\right) \ , \tag{13}$$

and C_f is the friction coefficient which is related to the pressure drop coefficient λ by:

$$C_f = \lambda/4 \ . \tag{14}$$

The pressures ate point 1 and point 2 are related by:

$$\frac{p_2}{p_1} = \frac{M_1}{M_2}\left(\frac{1+\frac{\gamma-1}{2}M_1^2}{1+\frac{\gamma-1}{2}M_2^2}\right)^{\frac{1}{2}} \ . \tag{15}$$

The mass flow rate in the pipe is then calculated by:

$$q_{tb} = A_p p_2 M_2 \sqrt{\frac{\gamma}{RT_2}} \ . \tag{16}$$

Fanno line differential model As we did for incompressible models, we can take into account the pipe dynamics by using a differential equation for the mass flow rate. In a similar way to Eq. 9, we obtain:

$$\dot{q_{tb}} = \alpha\left(q_{Fanno}^2 sign(p_t - p_b) - q_{tb}^2 sign(q_{tb})\right) \ , \tag{17}$$

where: q_{Fanno} denotes the flow obtained by Eq. 16;
α is a delay parameter $[kg^{-1}]$.

3 MODEL COMPARISON

In order to analyse the various pipe models and to show their limitations, we have integrated the bellow-tank equations for a simple test which consist in submitting the bellow to a crushing excitation. The bellow and tank properties are calculated using Eq. 4, Eq. 5 and Eq. 6. Varying the equation choosen for the pipe, we can compare four approaches as illustrated in the following table and confront them with the FLUENT results.

	Algebraic	Differential
Incompressible	Eq. 7	Eq. 8
Fanno	Eq. 16	Eq. 17

The bellow is submitted to a crushing-stretching sinusoidal excitation with a 20 mm semi-amplitude. The parameters of the model are listed in Tab. 1 where the pressure drop coefficient has been calculated with the Colebrook formula:

$$\frac{1}{\lambda} = -2.0\ log_{10} \frac{\epsilon/D}{3.7}\ . \tag{18}$$

Nominal bellow volume	V_{b0}	$11.6\ dm^3$	Initial pressure	p_0	$4\ bar$
Bellow volume gradient	dV_b/dz	$0.13\ m^2$	Initial temperature	T_0	$293\ K$
Effective area	A_e	$0.13\ m^2$			
Tank volume	V_r	$27\ dm^3$	Delay parameter		
Pipe length	L_p	$1\ m$	of Eq. 17	$alpha$	$1250\ kg^{-1}$
Pipe diameter	d_p	$18\ mm$			
Pipe wall rugosity	ϵ	$0.15\ mm$	Excitation semi-amplitude		$20\ mm$
Pressure drop coefficient	λ	0.03567			

Table 1: Parameters of the bellow-pipe-tank model

In the following sections, we first describe how the system has been implemented in the FLUENT software to obtain a reference solution. We then analyse the excitation frequency influence before showing the effects of the pipe length.

3.1 FLUENT model

The bellow-tank subsystem has been implemented and simulated with the FLUENT software. This model serves as a reference solution but it is too complex and time-consuming to be integrated in a model of the complete vehicle.

The model is based on an axisymetric approach considering both the bellow and the tank as cylinders aligned with the pipe axis. The geometrical parameters are identical to those given in Tab. 1 and the geometry is illustrated in Fig. 4. In this figure, the tank is on the left and the bellow is on the right. The moving mesh technique has been used. More precisely, the bellow displacement is modelled with the in-cylinder model (that is used for reciprocating engine modelling). The mesh is based on rectangular cells in that pipe and on triangular cells in the tank and the bellow. However, the cells adjacent to the moving boundary of the bellow are rectangular.

The flow is modelled using the standard $k - \epsilon$ closure for the turbulence. The standard wall modelling approach has been selected as it provides correct predictions for flows inside pipes.

a.

b.

c.

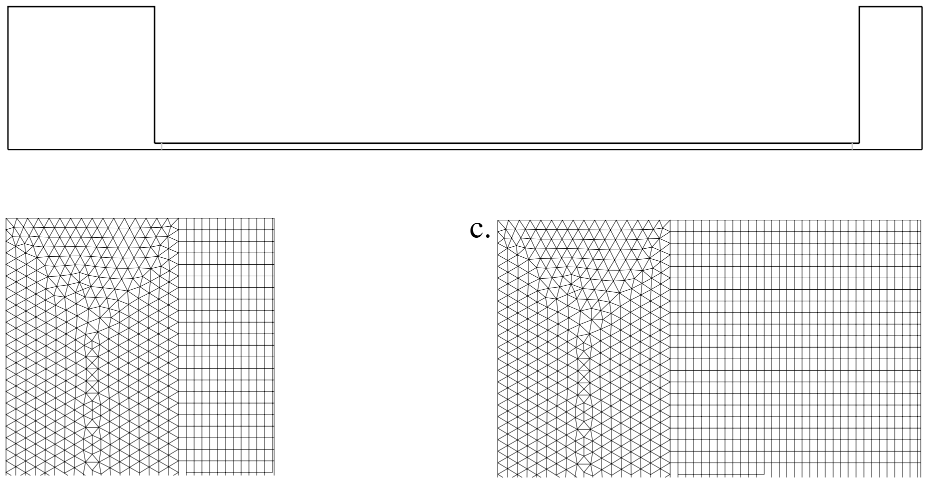

Figure 4: Illustration of the FLUENT model. a. Geometry of the system with the tank on the left and the bellow on the right. b. Partial representation of the bellow mesh for maximal crushing. c. Partial representation of the bellow mesh for maximal stretching.

The standard energy equation has been used including the viscous heating term in order to take into account the increase in average temperature observed in other models. The air inside the system has been considered as an ideal gas with constant properties.

The flow has been initialised with null velocity and the initial pressure. The equations have been solved using an explicit first order scheme in time and a second order scheme in space. The pressure has been recorded on the bellow and tank walls to compare them with the other models predictions. The mass flow rate in the pipe has been measured on both pipe ends (exactly at $10\ mm$ from the pipe connections with the tank and the bellow).

3.2 Comparison for various frequencies

For low frequencies, the four models agree well with the FLUENT curves as illustrated in Fig. 5. As the excitation is quite slow, the pressure in the tank "follows" the bellow pressure and therefore the pressure ratio is close to unity (about 0.96). The fluid velocity in the pipe is small and the compressible effects are negligible. The Mach number in the pipe does not exceed 0.13, value for which the incompressible hypothesis is satisfactory. This clearly appears in Fig. 6 that shows the impact of the pressure ratio on the steady state mass flow rate and the Mach number. For the FLUENT results, both the mass flow rates at point 1 and point 2 are plotted but they are too close from each other to be distinguished.

For higher frequencies, it is shown in Fig.7 that the mass flow curves of the algebraic models are in advance on the Fanno curve because they do not take the inertia of the fluid into account. We see that models with a differential equation for the pipe correctly capture this phase effect. On the other hand, the incompressible models present a larger oscillation amplitude than the reference results. Effectively, the tank pressure does not oscillate as much as the bellow pressure, the pressure ratio is thus lower (about 0.73), which induces greater fluid velocities in the pipe. The Mach number at end of the pipe is about 0.41 and compressible effects are no longer negligible. Those effects induce a mass flow limitation which is not taken into account by "in-

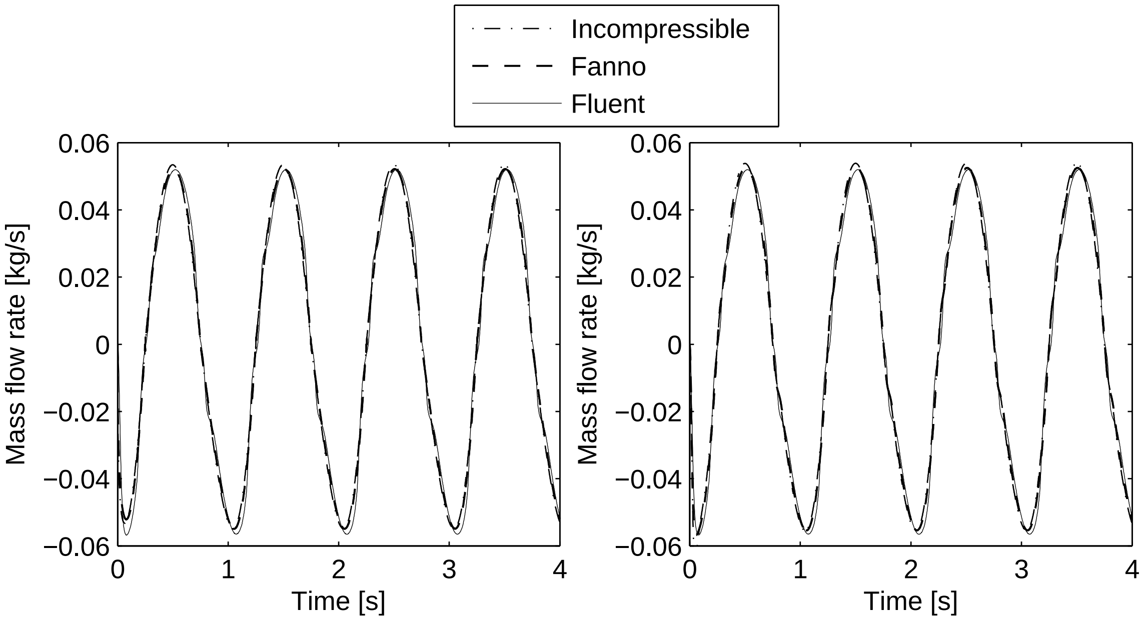

Figure 5: Mass flow rate for a 1 Hz excitation. Left: algebraic models compared with the FLUENT results. Right: differential models compared with the FLUENT results.

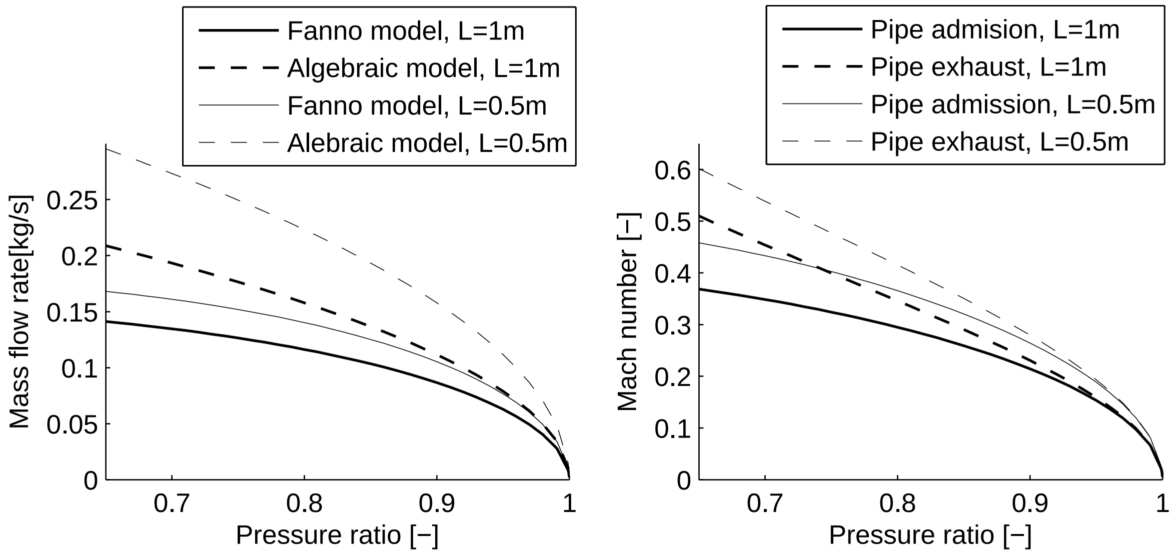

Figure 6: Left: influence of the pressure ratio on the steady state mass flow rate with the two models and for two different pipe lengths. Right: influence of the pressure ratio on the Mach number calculated with the Fanno model for two different pipe lengths.

compressible" models.The Fanno model with differential equation is the closest curve to the FLUENT results but still have a small amplitude error. In this case, we can distingish the two mass flow rate curves calculated by the FLUENT model: one corresponds to the flow entering in the bellow, the other to the flow exhausting from the auxiliary tank.

The influence on the pressure curves is more important for the tank than for the bellow because the bellow pressure variation is more guided by the volume variation than by the mass variation while the pressure variation in the tank depends only on the mass flow rate in the pipe.

The influence of the mass flow error on the bellow pressure does not seem too large. The bellow reaction force is therefore well approximated by the four models. The pipe model has more impact on the mass flow rate calculation, which could be of importance if an orifice or a valve was placed on the duct.

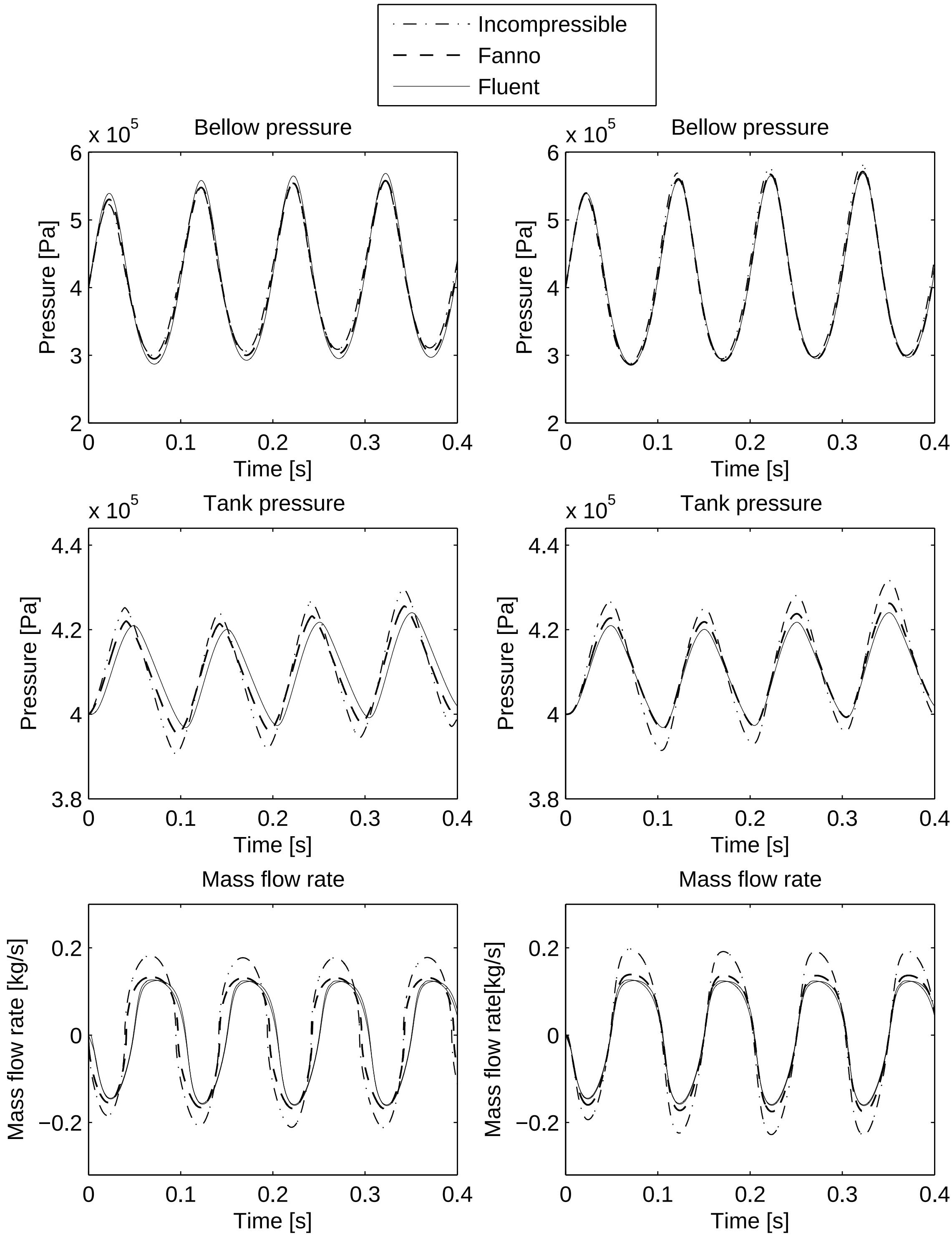

Figure 7: Pressure and mass flow rate for a 10 Hz excitation. Left: algebraic models compared with the FLUENT results. Right: differential models compared with the FLUENT results.

3.3 Influence of the pipe length

When reducing the pipe length, friction decreases and thus the fluid velocity is higher. The Mach number is about 0.48 at the pipe end even though the pressure ratio does not change compared with the case with a $1\ m$ long pipe. Therefore compressible effects become more important as depicted in Fig. 6. As illustrated in Fig. 8, the amplitue errors for incompressible models are more important.
The effects on the bellow pressure are more visible but they are still more important for the tank pressure. For the tank pressure the error seems to be smaller for the algebraic model than for the differential model, eventhough the differential model flow curves are closer from the FLUENT results.

4 CONCLUSIONS

This work illustrates the pneumatic pipe modelling within the context of railway pneumatic suspension. The pipe was analysed as a component of the bellow-tank subsystem for which several models were presented. We focused our attention on models for which it is possible to easily add valves and connections in order to be able to analyse every suspension topologies. For those models, we distinguished approaches which take algebraic equation for the pipe from those which use a differential equation. In a second step, we considered the Fanno model which does not neglect compressible effect but still derivates from a steady state hypothesis.
Those models were compared on a sinusoidal excitation test and confronted to axisymetric reference solution obtained with the FLUENT software. On the one hand this analyse highlights, for increasing excitation frequency, a phase difference on the mass flow rate time variation for the models which use an algebraic equation. On the other hand, it was shown that incompressible models overestimate the fluctuation amplitude of the mass flow rate. Compressible effects become no more negligible when frequency increases especially for shorter pipes.
The effects are not so important on the bellow pressure which mainly depends on the volume variation imposed by the excitation. However, the mass flow rate and the tank pressure are strongly influenced by the choosen model. We therefore will investigate the pipe model impact when an orifice or a valve is added to the system.
Those models will then be integrated into a complete pneumatic model and coupled with the train multibody model. We will thus analyse how the model refinement influences the global system performances with respect to the well-established comfort and safety railway criteria. This global approach is not restricted to the pipe modelling and will be extended to the other components of the pneumatic circuit such as the valves, in order to obtain a better understanding of the suspension behaviour and to be able to deal with novel suspension designs.

5 ACKNOWLEDGEMENTS

Nicolas Docquier is supported by the Fonds de la Recherche Scientifique - FNRS and gratefully acknowledge the *Multibody Dynamics 2007* Organizing Committee for the travel scholarship he was awarded to participate to the conference.

REFERENCES

[1] L. Sass. *Symbolic Modeling of Electromechanical Multibody Systems.* Louvain-la-Neuve (Belgium), January 2004.

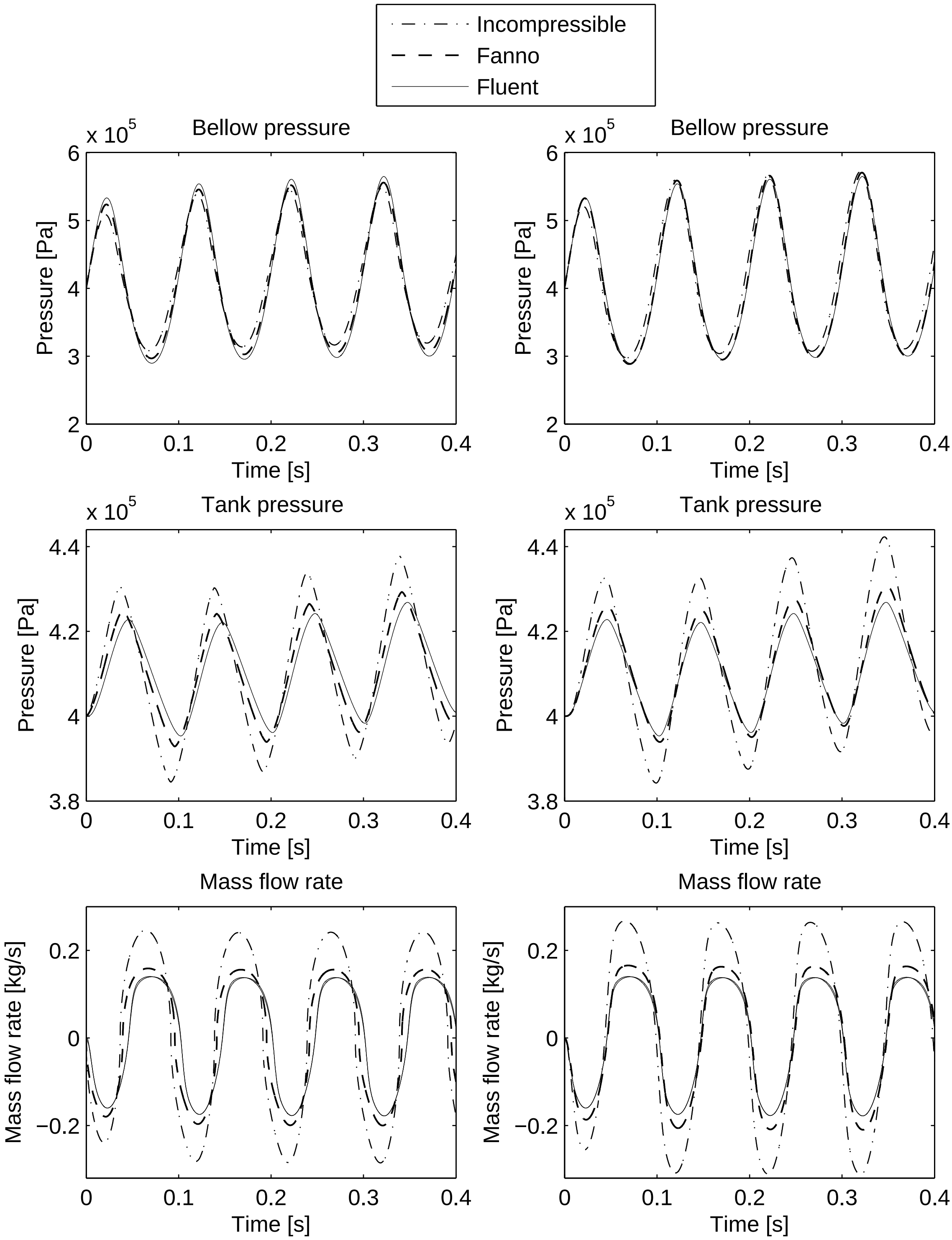

Figure 8: Pressure and mass flow rate for a 10 Hz excitation with a $0.5\ m$ pipe. Left: algebraic models compared with the FLUENT results. Right: differential models compared with the FLUENT results.

[2] M. Delannoy, P. Boon, B. Vandermissen, P. Fisette. Modelling hybrid multibody systems: application to vehicle hydraulic semi-active suspensions. Communication, *ECCOMAS - Multibody Dynamics 2005*, Madrid (Spain), 21-24, 2005.

[3] M. Berg. A three-dimensional airspring Model with friction and orifice damping. In: Pro-

ceedings of the 16th IAVSD Symposium on Dynamics of Vehicles on Roads and Tracks, Pretoria, South Africa, 1999. *Journal of Vehicle System Dynamics*, **33**, 528-539.

[4] INTEC GmbH, *Documentation to Simpack.* Simpack version 8.7 edition. 2005.

[5] N. Docquier, P. Fisette, H. Jeanmart. Multiphysic modelling of railway vehicles equipped with pneumatic suspensions. To appear in *Vehicle System Dynamics*.

[6] J. D. Anderson Jr. *Modern Compressible Flow With Historical Perspective.* McGraw-Hill, New York, 1990.

[7] J. D. Mattingly. *Elements of Gas Turbine Propulsion.* McGraw-Hill, New York, 1996.